LA-UR-17-31348
Approved for public release; distribution is unlimited.

Title: Water Diffusivity in Nitroplasticizer at Elevated Temperatures

Author(s): Yang, Dali

Intended for: Report

Issued: 2019-10-02 (rev.2)

Water Diffusivity in Nitroplasticizer at Elevated Temperatures

Dali Yang
MST-7, Material Science Technology Division
Los Alamos National Laboratory, Los Alams, New Mexico, 87545, U.S.A.

At elevated temperatures (T<55°C), the water diffusivity (D) in Nitroplasticizer (NP) is determined to be a function of the temperature given by the following Arrhenius law:

$$D(T) = A\, exp(-E_A/RT), \quad E_A = 62.8\frac{kJ}{mol}, \quad A = 3.716 \text{ x } 10^5 \text{ cm}^2/\text{sec}. \qquad (1)$$

This relation is obtained from the experimental results and the properties of the diffusion processes explained in the following.

Experiment Technique and Diffusion Equation

Water diffusivity in NP has been previously measured by Salazar et. al (2003) at room temperature.[1] Overall, the water solubility in NP is very low (<0.28 wt% at room temperature). When conventional gravimetrical method was used, one would have to use a large quantity of NP to be able to accurately measure the weight change during the water gain and loss. In this work NIR spectroscopy (Thermo Nicolet™ iS™ 50 FTIR spectrometer) is used to measure the water content. This technique is known be able to detect small changes in the water concentration in an organic liquid, since water has a unique peak in the NIR region (4000–10000 cm^{-1}). At a low water concentration, the intensity of the water peak obeys the Beer's law. From the peak intensity, the water concentration can be determined by using a calibration curve from a set of standard solutions. The water concentration in the standard solution was measured using Karl Fischer titration method (~98% of accuracy) (Mettler Toledo Instrument).

Water transport in NP can be described by the diffusion equation:

$$\frac{\partial C}{\partial t} = D\nabla^2 C\,, \qquad (2)$$

where C is the concentration at position x, y, z at time t, and D is the diffusivity. The experiments described in this report is designed to determine this diffusivity at different temperatures.

Short-term experiment

To characterize the uncertainties associated with the NIR spectroscopy technology and to independently verify the work of Salazar *et al.* (2007)[1], short-term experiments at the ambient condition are conducted. In the first experiment, an NIR fluid cell (22 mm in outer diameter and 1mm thickness) was half-filled with NP liquid, as shown in Fig. 1. The cell was opened to the ambient conditions for 1.5 and 2.5 hours. The NIR spectra were measured from top to bottom of the cell sequentially as illustrated in the figure. The water concentrations at different locations and at different times are plotted in the bottom portion of Fig. 2.

When $\sqrt{Dt}$ is much smaller than other relevant lengths of the fluid cell, we can treat the diffusion as one-dimensional that admits similarity solutions. For this experiment, we assume the concentration $C=C_{min}$ as the boundary condition on the NP-gas interface (~520 ppm). The solution of the concentration can be found as:

$$C(x,t) = (C_0 - C_{\min})erf(\frac{x}{2\sqrt{Dt}}) + C_{\min}\,, \qquad (3)$$

where C_0 is the water concentration in NP at the beginning of the measurement (~750 ppm). Using the experiment data, we then use eq. (3) to find the diffusivity (D) that fits the data the best. The results and errors are summarized in Table 1.

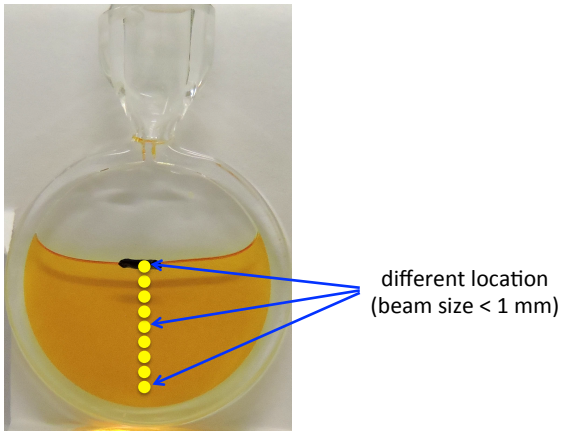

Figure 1. An illustration of an IR fluid cell with half-filled NP. The yellow dots indicate the locations NIR beam in the measurement. The fluid cell size is 20 mm in diameter and 1.0 mm in light path. The measurement was conducted at room temperature (21±2°C).

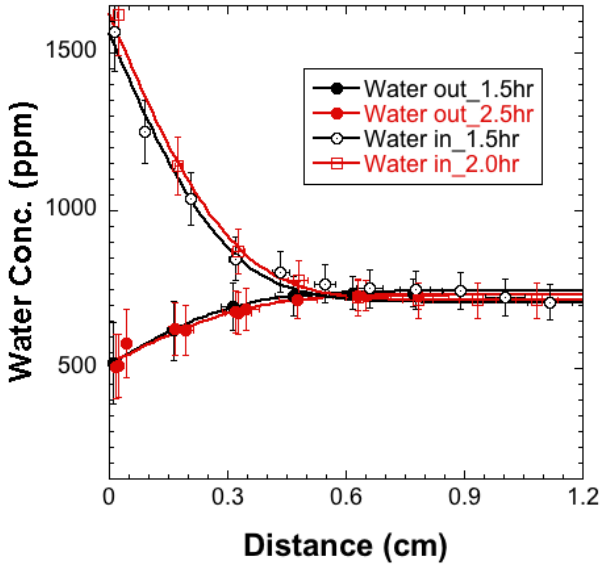

Figure 2. The water concentration changes with the location in two representative experiments. The points are the experimental data, and the lines are the fitted results using eq. 2 and eq. 4. The error bars suggest the potential errors during the measurement on the water concentration and location.

For this case, the fittings are reasonable but not convincing because of the errors. The main source of error is the measurement time. Since the measurement starts from top to bottom, strictly speaking, the spectra at different location were not collected at the same time. Furthermore, we assumed that the water concentration on NP-air interface is zero. This is an approximation since the cell has a narrow opening causing some resistance and small water concentration at the interface. The encouraging sign it that the calculated diffusivities are ~6.0 x10^{-6} cm^2/sec, which are very similar to the value [(5 ± 3) x 10^{-6} cm^2/sec] reported by Salazar *et al.* in 2007[1].

Table 1. Summary of experimental conditions, calculated diffusivity of water in NP, and the fitting parameters. Experimental temperature was 21±2 °C.

Experiment condition	Time (hour)	Diffusivity (e-6) (cm^2/sec)	C_{min} (ppm)	R^2
Water out	1.5	6.01	508.0	0.9991
Water out	2.0	5.95	514.2	0.9730
Water in	2.0	5.15		0.9822
Water in	2.5	4.91		0.9209

To better control the boundary condition, the other experiment was performed. Instead of letting the NP expose to the air, in this second experiment, water was added at the top of the NP liquid, as shown in Fig. 3. The NIR spectra data were collected from top to bottom of the cell after NP and water have been in contact for 2 and 2.5 hours. The water concentrations at different locations and at different times are plotted in the top portion of Fig. 2. For this case, the solution to eq. (2) becomes:

$$C(x,t) = (C_s - C_0)erfc(\frac{x}{2\sqrt{Dt}}) + C_0. \quad (4)$$

where C_s is the water saturation concentration at the water-NP interface and C_0 is the water concentration in NP at the beginning of the measurement (~750 ppm).

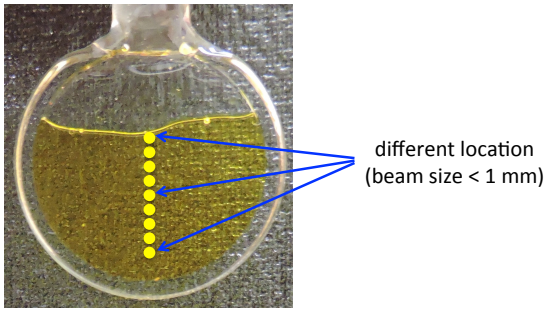

Figure 3. An illustration of an IR fluid cell with a half-filled NP and water added at the top portion of the cell. The yellow dots indicate the locations where the NIR beam line shines through during the measurement. The fluid cell size is 20 mm in diameter and 1.0 mm in length. The measurement was conducted at room temperature (21±2 °C).

Using this set of data, we again, find the diffusivity D that fit the experiment date the best. The results and calculation errors are also summarized in Table 1. The fit for this set of is much better than the water loss data because the boundary condition is better controlled. The values of R^2 are great (~0.92 to ~0.98). The calculated diffusivities are ~5.51 x 10^{-6} cm^2/sec, which are, again, similar to the value (5 ± 3) x 10^{-6} cm^2/sec reported by Salazar *et al.* in 2007.[1] The main sources of errors come from the following factors: 1). Water-NP surface is not flat; 2). Since the beam size is ~1 mm, it is very difficult to collect the spectrum at the exact interface between water and NP without having the effect from water phase; and 3). Similarly to the first experiment, the measurement was conducted sequentially from top to bottom. Strictly speaking, the spectra at different location were not collected at the same time. Despite many sources of errors, these experiments demonstrate that the NIR method can be used to determine the water diffusivity in NP with a reasonable accuracy.

Long-term solution:

To measure the diffusivity at elevated temperatures, we perform long-term experiments. The experiments were performed based on the following property of the diffusion process. The solution to eq. (2) can be written in terms of eigenfunctions of the Laplace operator ∇^2 as:

$$c(x,y,z,t) = \sum_{i=1}^{\infty} T_i(t) f_i(x,y,z), \tag{5}$$

where $f_i(x,y,z), i = 1, 2, \ldots$ are the linearly independent eigenfunctions of ∇^2,

$$\nabla^2 f_i(x,y,z) = -\lambda_i f_i(x,y,z). \tag{6}$$

Substituting (5) into (2) and noting the linear independence of the eigenfunctions, one finds

$$\frac{dT_i}{dt} = -\lambda_i D T_i, \quad \text{or} \quad T_i = \exp(-\lambda_i D t). \tag{7}$$

Therefore

$$c(x,y,z,t) = \sum_{i=0}^{\infty} \exp(-\lambda_i D t) f_i(x,y,z); \quad 0 = \lambda_0 < \lambda_1 < \lambda_2 < \ldots . \tag{8}$$

In this equation, negative eigenvalues of λ_i are not practically meaningful. At sufficiently large times (such that $\sqrt{Dt}$ is much greater than the largest length of the problems), only the first two terms in (8) are significant and the solution can be approximated by

$$c(x,y,z,t) \approx c_e(x,y,z) + \exp(-\lambda_1 D t) f_1(x,y,z). \tag{9}$$

After integrating (7) over the problem domain, one finds that the total mass of water approach its equilibrium value exponentially with time. This conclusion is the well-known Biot approximation or Newton's law of cooling in cases of thermal problems. We re-derive it here to show that: (1) the exponential decay toward the equilibrium is point wise [$Ce(x,y,z)=C_{min}$]; and (2) the decay rate is proportional to the diffusivity D, which is independent of the position in the problems domain although the eigenvalue λ_1 and eigenfunction $f_1(x,y,z)$ depend on the geometry and the boundary of the problem. It is important to note that these eigenvalues and eigenfunctions are independent of the diffusivity. For two systems with different diffusivities D and D', but with the same geometries and boundary conditions, the eigenvalue λ_1 and the eigenfunction $f_1(x,y,z)$ are the same, and the exponential decay rate is then related by

$$\frac{\lambda_1 D'}{\lambda_1 D} = \frac{D'}{D}. \tag{10}$$

Using this relation, if the diffusivity is known for one of the systems, we can determine the diffusivity of the other system by measuring the exponential decay rates, $\lambda_1 D$ and $\lambda_1 D'$.

The diffusivity at elevated temperature is determined by using the diffusivity at the ambient temperature as the reference, based on this mathematical property. For this mathematical property to be useful, it is important to enforce the same geometries and boundary conditions in the experiments. The small openings of the fluid cells make such enforcement possible. To quantify the error resulted from the boundary conditions, two sets of fluid cells are prepared: one set was capped with the air on the top while the other set was capped after the top was purged with nitrogen. They were placed inside a PTFE container and then the containers were placed in five ovens with the temperature setting at 38, 45, 55, 64, and 70 °C, while one cell was kept at the room

temperature. Periodically, the NIR spectra of these samples were collected at the center of the cells right after they were removed from the oven. Fig. 4 shows photos of the fluids cell taken after the specific days in the ovens. Water concentration changes over time for both sets are shown in Fig. 5. Clearly, the water concentration decays exponentially with increasing time as predicted by eq. (9). The decay rate $\lambda_1 D$s at different temperatures are listed in Table 2. With the known diffusivity of water at the room temperature, eq.(10) is used to calculate the diffusivity of water in NP at the elevated temperatures.

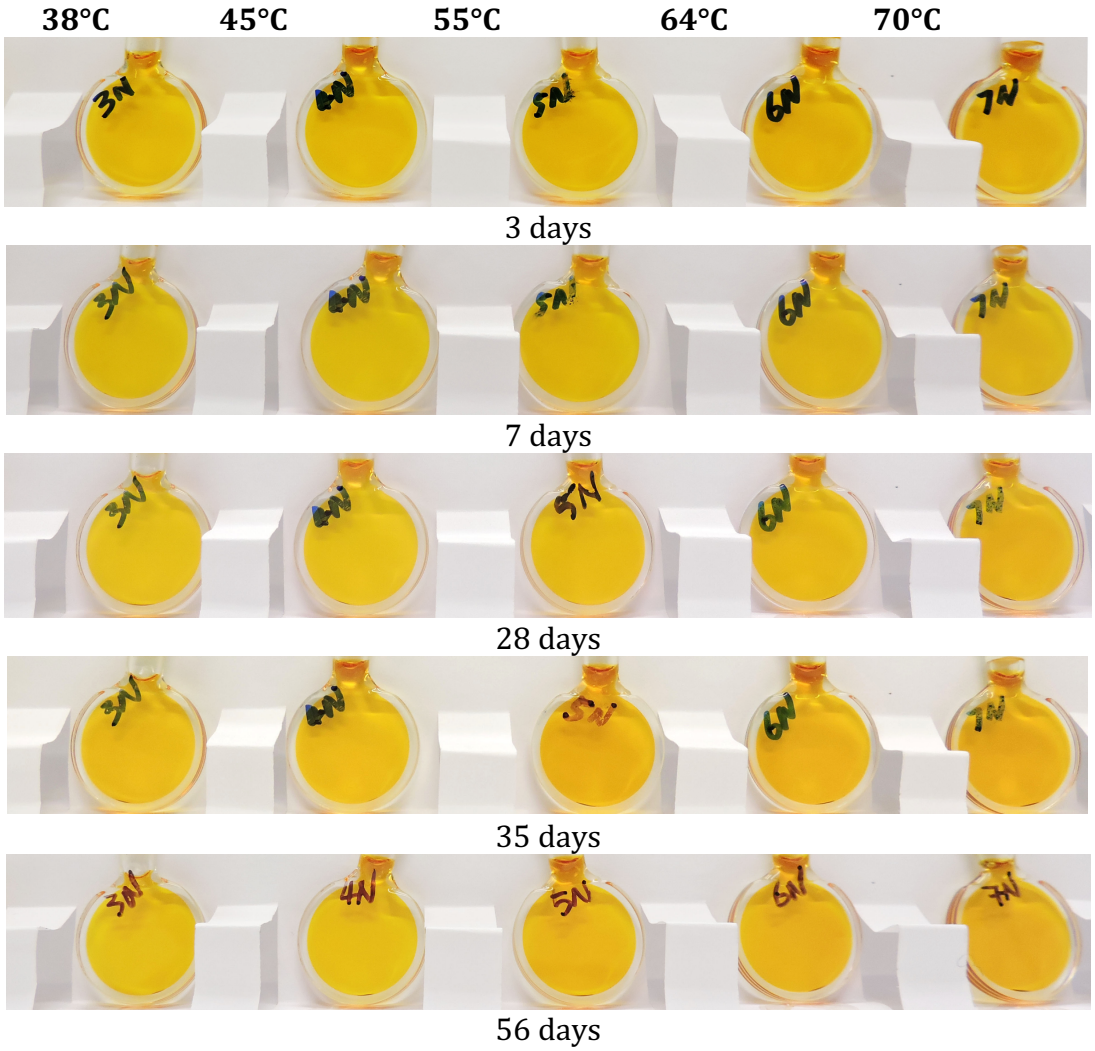

Figure 4. The photos of the fluid cells after they had been heated at different temperatures for different times. The appearances of the Air set of samples are very similar to those obtained from the N_2 set of samples.

Figure 5 shows that the rate of water decay increases as the temperature increases when the temperatures are lower than 55°C. However, as the temperature further increases, the rates of water decay at 64 and 70°C in both the Air and N_2 sets are even lower than or similar to that obtained from the 55°C condition. From the photos in Fig. 4, one notices that the NP color in the 64 and 70°C cells becomes slightly darker than that in the low temperature cells. The NIR and middle IR results also show newly emerged peaks. These observations suggest that at temperatures above

55°C, there are mechanisms other than diffusion affecting the water concentration in this experiment. These mechanisms will be studied in the future. For the samples heated below 55°C, other characterizations, such as FTIR and TGA, suggest that their properties show insignificant changes within the two-month experimental period. These results allow us to assume that the concentration changes in these samples are mainly due to the water diffusion. For these samples using eq. (10), the water diffusivities at 38, 45, and 55°C are obtained. The results are summarized in Table 2.

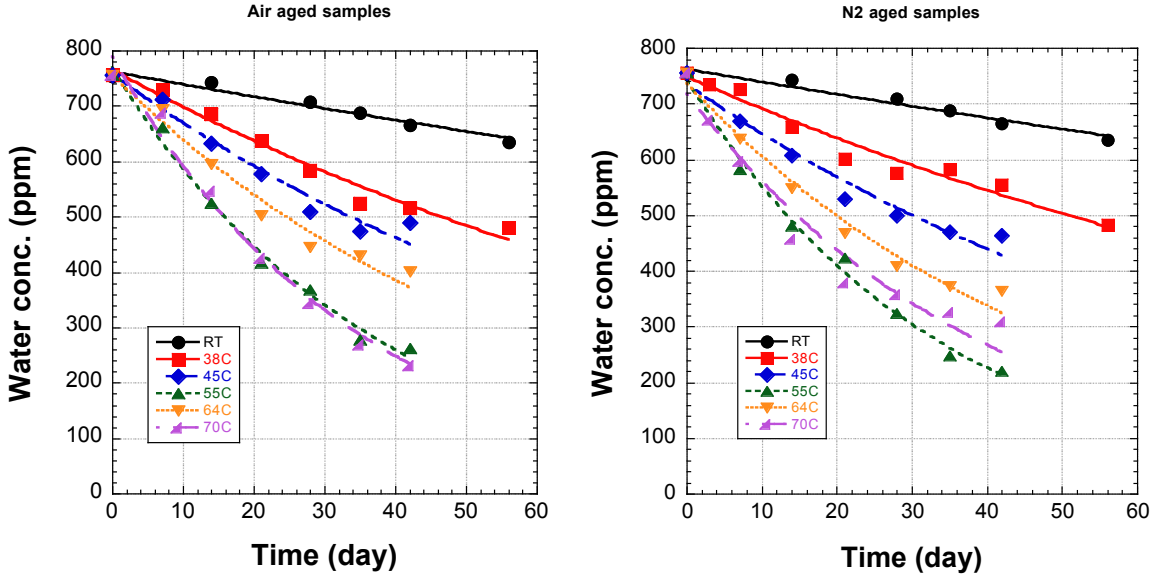

Figure 5. The water concentration changes over heating times at the center location of the cells. The points are the experimental data, and the lines are the fitted results using eq. 7.

Table 2. Summary of experimental conditions, calculated diffusivity of water in NP, and the fitting parameters. Experimental temperature ranges from 22 to 70°C.

Temperature (°C)	$\lambda_1 D$	R^2	Diffusivity (e-6) (cm^2/sec)
	Air set		
21.5	0.003204	0.9701	4.10
38	0.009030	0.9746	11.55
45	0.01303	0.9612	16.67
55	0.02710	0.9911	34.65
	N2 set		
21.5	0.003204	0.9701	4.10
38	0.007954	0.9613	10.17
45	0.01361	0.9597	17.41
55	0.02982	0.9922	38.13

The similar values of diffusivities for the N_2 set and the air set provide a posterior validation of the assumption about the same boundary conditions. The water diffusivity increases more than 8 times as the temperature increases from ~21 to 55°C. Based on the diffusivity values in Table 2, we find the diffusivity can be related to the temperature using the Arrhenius law (1) and is plotted in Fig. 6.

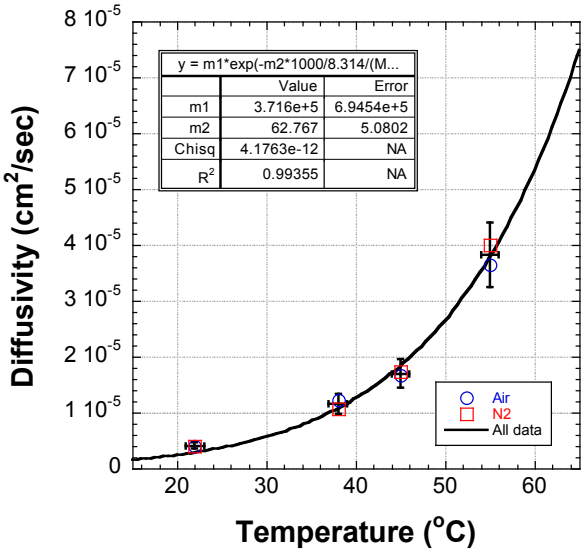

Figure 6. The calculated diffusivities of water in the NP phase at different temperatures. Points are the experimental data, and solid line is the Arrhenius fitted line based on the data points obtained from both the Air and N_2 sets of experiments.

As shown in Fig. 6, the Arrhenius law, eq. (1), represents the data quite well despite many uncertainties in the experimental procedure. These uncertainties include the boundary conditions. As shown in Fig. 4, despite the best effort, it is not possible to experimentally ensure the boundaries in the fluid cells are exactly identical. When the NIR spectra were collected, one empty cell was used to calibrate the background for all cells. Errors can be introduced because of difference among these cells. Although the measurements are done right after the samples are taken out of the ovens, measurements take times, hence the actual temperatures at the measurement were typically lower than the oven temperatures. As a consequence, the error at a higher temperature is greater than that at a lower temperature. Furthermore, the water concentrations of the samples were converted from the calibration curve constructed from the KF titration results of a set of standards, which also contains error.

Acknowledgement

Author thanks Justine Yang for help on the NP sample preparation and the KF measurement. This work was supported by the US Department of Energy through the Los Alamos National Laboratory Enhanced Surveillance Programs.

References:

1. Salazar, M. R.; Thompson, S. L.; Laintz, K. E.; Meyer, T. O.; Pack, R. T. *Journal of Applied Polymer Science* **2007,** 105, 14.